

Bismuth Improvements on the Mechanical Performance of an As-Cast Eutectic Sn-Cu Alloy

Mohammed S. Gumaan (*,1)

© 2024 University of Science and Technology, Sana'a, Yemen. This article can be distributed under the terms of the [Creative Commons Attribution License](#), which permits unrestricted use, distribution, and reproduction in any medium, provided the original author and source are credited.

© 2024 جامعة العلوم والتكنولوجيا، اليمن. يمكن إعادة استخدام المادة المنشورة حسب رخصة مؤسسة المشاع الإبداعي شريطة الاستشهاد بالمؤلف والمجلة

¹ Biomedical Engineering Department, Faculty of Engineering, University of Science and Technology, Sana'a, Yemen

* Corresponding author: m.gumaan1@gmail.com

Bismuth Improvements on the Mechanical Performance of an As-Cast Eutectic Sn-Cu Alloy

Abstract:

The eutectic Sn-Cu alloy considered one of the potential alternatives to the toxic Sn-Pb solder alloys. This work aims to improve the mechanical performance of the eutectic Sn-Cu alloy in terms of rupture time and creep properties through studying the effects of bismuth (Bi) and silver (Ag) contents with $x = 0.3$ and 0.5 wt.% for each on the mechanical properties of as-cast eutectic Sn-Cu alloy. Ternary as-cast Sn-Cu-X ($X = \text{Bi}$ or Ag) alloys were investigated using x-ray diffractions (XRD) and Creep testing machine. The results revealed that the 0.3 and 0.5 wt.% of Bi additions to the as-cast eutectic Sn-Cu alloy do not promote the Cu_6Sn_5 IMC formation but just shifted it from 102 to the 202 orientations. The above-mentioned Bi additions have refined the β -Sn particle size and enlarged Cu_6Sn_5 IMC, thus reduced the lattice distortion that is directly enhanced the mechanical performance and reliability for these as-cast alloys through the tensile tests with different loads at room temperature (RT). Adding 0.3 and 0.5 wt.% of Bi to the as-cast eutectic alloy formed other IMC (Ag_3Sn) alongside the Cu_6Sn_5 phase which is mismatched with it due to their different crystal structures (Ag_3Sn (orthorhombic) and Cu_6Sn_5 (Hex)). For that, the structural stability decreased, which leads to low resistance for the external forces and low mechanical reliability. The mechanical improvements (high rupture time (5498.85 s), low strain rate, and stress exponent (9.48)) that have been reported with the 0.5 wt.% of Bi addition to the as-cast eutectic alloy which is strongly related to its high structural stability compared to that for the other additions. From the mechanical point of view, the Sn- 0.7Cu - 0.5Bi alloy is recommended to be the most mechanical reliable alloy for the large-scale production and processing soldering and electronic assembly.

Keywords: as-cast eutectic Sn-Cu, rupture time, stress exponent, mechanical performance, particle size, IMC.

تحسينات البزموث على الأداء الميكانيكي لسبيكة القصدير-نحاس Sn-Cu سهلة الانصهار

الملخص:

تعتبر سبيكة Sn-Cu سهلة الانصهار أحد البدائل المحتملة لسبائك اللحام Sn-Pb السامة. يهدف هذا العمل إلى تحسين الأداء الميكانيكي لسبيكة Sn-Cu سهلة الانصهار من حيث زمن التمزق وخواص الزحف من خلال دراسة تأثير محتوى البزموث (Bi) والفضة (Ag) بنسبة $x = 0.3$ و 0.5% وزن لكل منهما. الخواص الميكانيكية لسبائك Sn-Cu سهلة الصب. تمت دراسة السبائك الثلاثية Sn-Cu-X (Ag أو X = Bi) باستخدام حيود الأشعة السينية (XRD) وآلة اختبار الزحف. كشفت النتائج أن 0.3 و 0.5% بالوزن من إضافات Bi إلى سبيكة Sn-Cu سهلة الصب لا تعزز تكوين IMC Cu_6Sn_5 ولكنها حولته من 102 إلى الاتجاه 202. لقد أدت إضافات Bi المذكورة أعلاه إلى تحسين حجم الجسيمات β -Sn وتوسيع Cu_6Sn_5 IMC، وبالتالي تقليل تشويه الشبكة الذي يعزز بشكل مباشر الأداء الميكانيكي والموثوقية لهذه السبائك المصبوبة من خلال اختبارات الشد بأحمال مختلفة في درجة حرارة الغرفة. أدت إضافة 0.3 و 0.5% بالوزن من Bi إلى السبائك المصبوبة سهلة الانصهار إلى تشكيل $IMC (Ag_3Sn)$ إلى جانب الطور Cu_6Sn_5 الذي لا يتطابق معه نظرًا لبنيتها البلورية المختلفة (Ag_3Sn) (المعيني) و (Cu_6Sn_5) (Hex). ولهذا انخفض الثبات الهيكلي مما يؤدي إلى انخفاض المقاومة للقوى الخارجية وانخفاض الموثوقية الميكانيكية. التحسينات الميكانيكية (وقت التمزق العالي (5498.85 ثانية)، ومعدل الإجهاد المنخفض، الإجهاد (9.48)) التي تم ذكرها مع إضافة 0.5% بالوزن من Bi إلى السبائك سهلة الانصهار المصبوبة والتي ترتبط بقوة بارتفاعها الاستقرار الهيكلي مقارنة بالإضافات الأخرى. من وجهة النظر الميكانيكية، يوصى بأن تكون سبيكة Sn- $0.7Cu-0.5Bi$ هي السبائك الأكثر موثوقية ميكانيكية للإنتاج على نطاق واسع ومعالجة اللحام والتجميع الإلكتروني.

الكلمات المفتاحية: : سبيكة سهلة الانصهار Sn-Cu، زمن الانقطاع، الإجهاد، الأداء الميكانيكي، حجم الجسيمات، الطور المركب البيني.

1. Introduction

Lead-free solder alloys are typically Sn-based alloys due to the high corrosion resistance and good solderability of tin (Sn) [1]. Solder alloys based on the eutectic Sn–Ag and Sn–Cu alloy systems have been found to be amongst the most favorable lead-free alternatives [2][3][4] [5][6][7]. Although the Sn–Ag and Sn–Ag–Cu solders are the most widely studied solder systems because of their high strength, creep resistance, and excellent machinability. However, due to their high cost, they can not be applied to large-scale production and processing [8]. This leads to more extensive research to develop the eutectic Sn–Cu alloy. F. TAI et. al [9] have studied the nanosized Ag reinforcements on the mechanical performance, and creep-rupture behavior of the Sn–0.7Cu solder. They revealed that the composite solders and their joints showed better wettability and mechanical properties, as well as longer creep-rupture lives than Sn–0.7Cu solder. J. Shen et. al [10], have investigated the influence of the cooling rate and Cu content on the microstructures of the solidified Sn–Cu alloys. They observed bulk Cu₆Sn₅ intermetallic compounds (IMCs) formed only in the Sn–1.0Cu alloy with lower cooling rate whereas at a higher cooling rate, the actual eutectic point of Sn–Cu solder alloy shifts to the direction of higher Cu concentration. Meng Zhao et. al [11] have improved the Sn–Cu lead-free solders performance by alloying, particle strengthening, optimization of the soldering process, and development of matching soldering fluxes. They confirmed on the essentiality to understand the structure-performance relationships and potential reliability problems of Sn–Cu solders. They also recommended investigating new Sn–Cu based solders for specific electronic components. Li Yang et. al [12] have studied the aluminum effects on the microstructure and mechanical properties of Sn–0.7Cu–xAl (x = 0–0.075) solder alloy, they found that the IMCs in the Sn–Cu–Al solder alloy is varied from Cu₆Sn₅ in the Sn–Cu–(0.01–0.025)Al to Al₂Cu in the Sn–0.7Cu–(0.05–0.075)Al. They suggested Sn–0.7Cu–0.075Al is an optimized lead-free solder alloy for the copper substrate. The 0.2% proof stress and tensile strength are less than the values for an Sn–0.7Cu binary alloy with adding 1 mass% of Ag to the eutectic Sn–Cu alloy according to S-H. Huh, et. al [13]. Mevlüt Şahin et. al [14] are determined the relationships among phase spacings, solidification rate, and mechanical properties from linear regression analysis for the Sn–36Bi–22Cu (wt.%) ternary eutectic alloy. The influence of Ag and In additions on tensile creep behavior and thermal properties of bulk eutectic Sn–Cu solder alloy is reported by El-Daly et. al

[15]. The creep strain rate increases and creep lifetime decreases as the applied stress level and temperature increase. By more research, it has been noticed that there are no further studies that investigate the creep deformation mechanism through stress exponent and rupture time of the eutectic Sn-Cu alloy. The eutectic Sn-Cu alloy is considered one of the potential candidates for tin-based lead-free solders. It has the lowest cost among several kinds of lead-free solder at present [16]. It is easy to produce and recover and can inhibit the dissolution of the copper matrix in immersion welding and wave soldering. However, the mechanical properties and wettability of that solder alloy are poor. At the same time, Sn-0.7Cu solder is more susceptible to electric corrosion due to the potential difference between Sn and Cu [17]. Generally speaking, the Sn-Ag-Cu and Sn-Cu alloys have their own advantages and disadvantages, but compared with each other, the performance of Sn-Ag-Cu is better, but the low-cost Sn-Cu has more advantages. So, the aim of this study is to improve the mechanical performance of an as-cast eutectic Sn-Cu alloy through a series of microstructural modifications resulted from small additions of Bi and Ag.

2. Experimental procedure

2.1. Materials preparation

Two various concentrations of each bismuth (Bi) and silver (Ag) contents (as 0.3 and 0.5 wt.%) were selected as doping additions to the eutectic as-cast Sn-Cu alloy. The purity of all Sn, Cu, Bi, and Ag elements is about 99.95%. The five as-cast ternary Sn-Cu-X (X= Bi or Ag) alloys systems studied were, using an electric furnace at 650 °C and inside the Pyrex tub, melted. They were manually agitated at approximately 200 °C above their melting points to achieve homogenization. Then shaken them to ensure homogenization of the melt and then left to solidify slowly to room temperature (RT) in order to obtain samples containing the fully precipitated phases, after that the Pyrex tub was broken to obtain the sample. The cast ingots obtained were rolled drawn into wires of one mm diameter and 60 mm length for the structural analysis and creep resistance. The samples were polished using grades of silicon paper and then washed in a solution of (CH₃COCH₃). In order to remove residual stress and defects induced during specimen forming, the samples were annealed at 100 °C for 6 hours and then left to cool slowly to RT.

2.2. Materials investigation

X-ray Shimadzu EDX-720 model with CuK α radiation ($\lambda=1.54056 \text{ \AA}$) was used for XRD analysis. The XRD curves of the samples were constructed in the 2θ range of $5\text{--}75^\circ$. The source was operating under an accelerating voltage of 40 kV with a tube current of 20 mA. Continuous scanning was done with a constant scanning rate of 0.02/1sec. The tensile creep tests were implemented on all samples at different constant loads (18.7 and 21.2) MPa using a computerized vertical tensile technique. Every specimen was stretched until the fracture under the load effect at RT. The sample placed between the force sensor and a rotary motion sensor. Began the sample in vertical elongation, and recorded the value of strain with time using a rotary motion sensor. Then the power link can transport data from sensors to data Studio Software in the computer.

3. Results and discussion

3.1. Structural analysis

Fig. 1 shows the x-ray diffraction (XRD) curves for as-cast Sn–0.7Cu–xBi or Ag solders with $x = 0, 0.3, \text{ and } 0.5$ respectively. This figure is considered as a map for the IMCs' positions, orientations, and concentrations whereas all the undefined peaks indicate to the β -Sn phase. Although J. Shen et. al [21] confirmed that following the equilibrium solidification process, the Cu $_6$ Sn $_5$ crystals can not be formed in Sn–0.7Cu alloy at lower cooling rates which could be determined by "lever rule" according to the phase diagram [22], An as-cast eutectic Sn-Cu solder displays two peaks due to Cu $_6$ Sn $_5$ dispersed in Sn-matrix. This indicates a partial dissolving for Cu content inside Sn-matrix but the undissolved Cu atoms reacted with the Sn atoms to form Cu $_6$ Sn $_5$. This may be because the as-cast eutectic alloy experience a metastable pseudoeutectic solidification route instead. With the additions of 0.3 and 0.5 wt.% of Bi to the eutectic Sn-Cu alloy, only Cu $_6$ Sn $_5$ (102) shifted to the Cu $_6$ Sn $_5$ (202) whereas no additional peaks for Cu $_6$ Sn $_5$ have appeared. The particle sizes for β -Sn and Cu $_6$ Sn $_5$ in all the as-cast Sn–0.7Cu–xBi/Ag solders were calculated according to Scherer Formula [23]:

$$t = (0.9 \lambda / B \cos \theta_b) \quad (1)$$

where: B is the broadening of diffraction line measured at half its maximum intensity (radians), t is the diameter of crystal particle, θ_b is the Bragg angle and λ is the wavelength of x-ray. From table 1, it has been noticed that the

particle size of β -Sn has been decreased with the Bi additions, whereas the size of Cu₆Sn₅ increased. Bi atoms work as barriers for β -Sn growth through the solidification process, which leads to the β -Sn reduction. The above-mentioned mechanism can be confirmed through the increased Cu₆Sn₅ sizes where it could attribute to the eutectic Cu₆Sn₅ phases, which cling to the primary Cu₆Sn₅ crystal during the eutectic reaction due to their matching crystalline orientation relationship [21]. Regarding the 0.3 and 0.5 wt.% of Ag additions, only two peaks due Ag₃Sn have appeared alongside the Cu₆Sn₅ peaks as shown in Fig. 1. The last addition (0.5 wt.% of Ag) cause to shift Cu₆Sn₅ IMC (at $2\theta = 42.8^\circ$) from (102) orientation to (202) orientation at ($2\theta = 62.5^\circ$). It is good to mention that the shifted Cu₆Sn₅ IMC cause to slightly decreased lattice distortion (1.20×10^{-3}) in the β -Sn matrix [24]. The β -Sn particle size has also decreased with Ag additions whereas the Cu₆Sn₅ size has increased. It is noticeable that the cell volumes for all as-cast alloys have been decreased with Bi and Ag additions as shown in Table 1. The lattice distortions were calculated according to G. K. Williamson and W. H. Hall [25]:

$$B = \left(\frac{1}{D_{eff}} \right) + 5 \leq \epsilon^2 \geq^{1/2} \sin \frac{\theta}{\lambda} \quad (2)$$

where: D_{eff} is the crystallite size, and ϵ is local lattice distortion in the β -Sn matrix.

A slight change has been occurred in (c/a) values from (0.540) to (0.549) due to a lattice expanding in a and c-axes with Bi and Ag additions. This distortion leads to raising the number of atoms per unit cell (N) slightly, which indicates to lattice line defects. The increased particle size of Cu₆Sn₅ IMC (30.54nm) with 5wt.% of Bi reduced the lattice distortion ϵ to (1.16×10^{-3}). The details of the XRD analysis shown in Table 1.

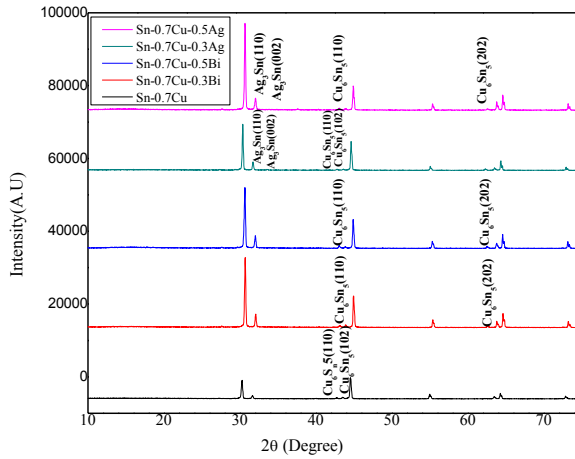


Figure 1: XRD patterns of the as-cast Sn-Cu-X (X= Bi or Ag) alloys

3.2. Mechanical and creep behaviour

With the development and miniaturization of electronic devices and surface mount technology, lead-free solders to be used in microelectronics industries are required to have excellent mechanical performance and high reliability, with elegant creep resistance, considered a necessity. Mechanical performance plays a vital role in the strength of any solder joints. Although the solder volume, joint geometry, bonding process, and solidification rate have different effects on mechanical properties, the most essential factor is the alloy composition of solder [9]. The effects of different Bi and Ag additions doping on the mechanical properties of Sn-Cu solder alloys were discussed, in terms of stress exponent, rupture time values, and creep behaviour. Depending on the structural parameters, the concentration and orientation of IMCs that are formed in the as-cast alloys are strongly related to the Bi and Ag additions. The structural stability of any alloy system is directly reflected in mechanical performance depending on the bonding nature among constituent atoms [26]. Fig. 2 a, b, c, d, and e shows the strain behavior with creep time for all the as-cast alloys. This test was implemented with different loads (1.5 and 1.7 kg) at RT. For all sub-figures 2, it has appeared that the strain rate with the highest load (1.7 kg) is more than that with the other load (1.5kg), which is returned to the pressure ratio per unit area [27]. In general, the rupture time (t) of the alloys with a 1.7 kg load is less than that with a 1.5 kg load. This time contraction is attributed to the increased force per unit area, thus atomic bonding, leading to the unbalancing energy in the

system that leads to the rupture rapidly. Comparison among fig 2 a, b, and c indicates to prolonged rupture time with adding 0.3 and 0.5 wt.% of Bi to the eutectic Sn-Cu alloy with both 1.5 and 1.7 kg loads as shown in Table 2. The rupture time improvements with these additions are strongly related to the refined particle size of β -Sn (table 1) [28] [29]. It is well known that the lower particle size alloy is more surface area exposed to the tension force, thus more possible chances of the atomic bonds to uniformly contribute through the tension process [30]. The more contributed atomic bonds mean more resistance to being ruptured. From fig 2 c, it is presented that the rupture time of as-cast Sn-0.7Cu-0.5 Bi alloy with 1.7 kg load is the longest compared to that of the eutectic Sn-Cu and Sn-0.7Cu-0.3 Bi alloys. The reason is may be returned to its lower lattice distortion (1.16×10^{-3}). Although the enhanced rupture time of the as-cast Sn-0.7Cu alloys with Ag additions, their values for rupture time still lower than that for Bi additions as shown in fig 2 and table 2. The reason is may be due to the low compatibility among Cu₆Sn₅ (Hex) and Ag₃Sn (Orthorhombic) phases which is basically returned to their different crystal structures [11]. The mismatching unlike crystal structures leads to the unstable building structure, which can be distorted with a little external force rapid than the stable phases [31]. Fig 3 shows the compared the strain behavior and rupture time for all as-cast alloys at 1.5 and 1.7 kg loads respectively. It can be concluded that the strain rate and rupture time of the eutectic Sn-Cu alloy have been improved with 0.3 and 0.5 wt.% of Bi additions whereas the opposite trend has appeared with 0.3 wt.% of Ag. This is related to the reduction of the particle size and lattice distortion of β -Sn [20]. With applying 1.7 kg load as shown in fig 3 b, it has appeared that the Sn-0.7Cu-0.5Bi as-cast alloy offers the highest rupture time (5498.85 s) and lowest strain rate compared to all other alloy compositions. These mechanical improvements are attributed to the high structural stability of that alloy compared to the other alloys. The low particle size (34.24 nm), absence of other types of IMCs (like Ag₃Sn), and low lattice distortion (1.16×10^{-3}) of Sn-0.7Cu-0.5Bi as-cast alloy may play a vital role to enhance its structural stability. Table. 2 shows the stress exponents (n) for all as-cast alloys which calculated according to the following equation [32]:

$$\varepsilon = A \sigma^n e^{\left(\frac{-Q}{RT_a}\right)} \quad (3)$$

where A is a structure-dependent constant, σ is the applied stress, n is the stress exponent, Q is the creep activation energy, R is the universal gas constant and T_a is the aging temperature in Kelvin. A straight line would be obtained from plotted creep rate against applied stress, σ on a double logarithmic scale as shown in Fig. 4, whose slope gives the stress exponent. The values of the stress exponent for the as-cast Sn-Cu- X ($X = \text{Bi}$ or Ag) alloys were taken as average with the 1.5 and 1.7 kg loads and tabulated in Table 4. From this table, it is remarked a slight reduction in the stress exponent with Bi additions whereas a significant reduction has been reported with Ag additions, especially with 0.3 wt.%. Stress exponent (n) is a more important factor that can indicate to the predominant deformation mechanism for any alloy system [33]. The stress exponent reported in the literature for metal alloys can be classified according to A. La Torre et. al [34] as Diffusion creep is associated with the n values around 1, grain boundary sliding leads to n values close to 2 and mechanisms attributed to dislocation movement such as slip creep are linked to n values in the range of 5-7 which moves up to higher values than 8 when particles reinforcement takes place. According to the above-mentioned data, it can be said that the suggested predominant creep mechanism for the as-cast eutectic Sn-Cu, Sn-0.7Cu-0.5Bi, and Sn-0.7Cu-0.5Ag alloys is the particles reinforcement whereas the dislocation movement (slip creep) controlling mechanism for the as-cast Sn-0.7Cu-0.3Bi alloy. It can be said that the as-cast Sn-0.7Cu-0.3Ag alloy is deformed according to the grain boundary sliding mechanism. This creep improvement with a 0.5 wt.% of Bi and other mechanical improvements make this alloy more resistant for the mechanical deformations, thus more mechanical reliability in electronic devices and packaging assembly compared to the as-cast eutectic Sn-Cu and other systems. So, and from the mechanical point of view and by the comprehensive comparison among all as-cast alloys, the Sn-0.7Cu-0.5Bi alloy recommended to be the best mechanical reliable alloy for the electronic devices and packaging assembly applications.

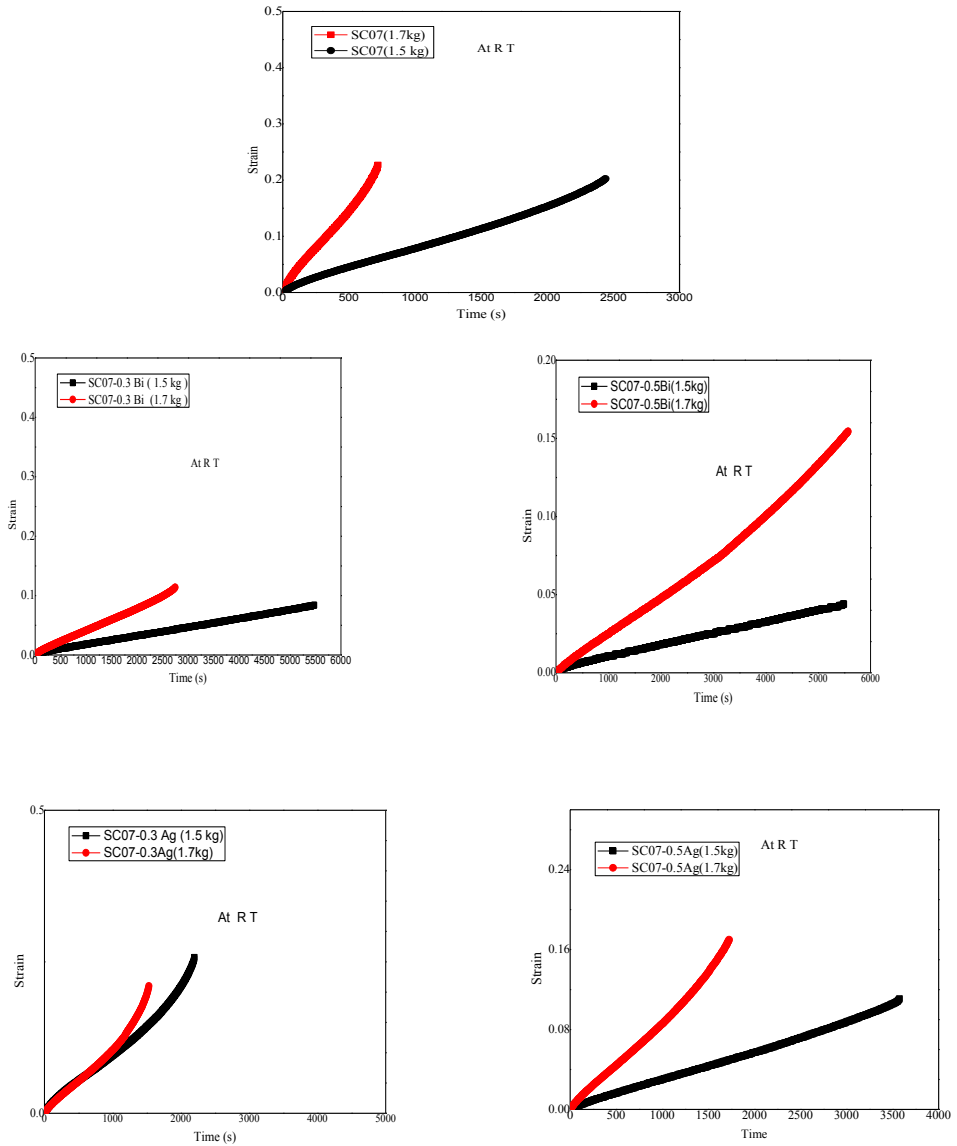


Figure 2: Creep curves of the as-cast Sn-Cu-X (X= Bi or Ag) alloys

Table 2: Mechanical and Creep parameters

Alloy in wt.%	Load (kg)	Rupture time (s)	Stress exponent (n)	Elongation (cm) %
SC07	1.5	2453.69	9.8	20.5
	1.7	738.23		22.97
SC07-0.3Bi	1.5	5498.85	7.5	8.48
	1.7	2780.47		11.55
SC07-0.5Bi	1.5	5498.85	9.48	4.47
	1.7	5498.85		15.33
SC07-0.3Ag	1.5	2226.21	1.5	25.99
	1.7	1539.61		21.33
SC07-0.5Ag	1.5	3615.30	8.9	11.24
	1.7	1736.14		17.25

4. Conclusions

To improve the mechanical performance of as-cast eutectic Sn-Cu solder alloy for the large-scale production and processing electronic applications, in terms of rupture time and stress exponent, depending on the structural changes in the solder alloys, the Bi/Ag effects on the eutectic Sn-Cu have been investigated. The results revealed that the 0.3 and 0.5 wt.% of Bi additions to the as-cast eutectic alloy do not promote the Cu₆Sn₅ IMC formation but just shifted it from 102 to the 202 orientation. The above-mentioned Bi additions have refined the β-Sn particle size and enlarged Cu₆Sn₅ IMC, thus reduced the lattice distortion that is directly enhanced the mechanical performance and reliability for these as-cast alloys. Adding 0.3 and 0.5 wt.% of Bi to the as-cast eutectic alloy formed other IMC (Ag₃Sn) alongside the Cu₆Sn₅ phase which is mismatched with it due to their different crystal structures (Ag₃Sn (orthorhombic) and Cu₆Sn₅ (Hex)). For that, the structural stability decreased which leads to low resistance for the external forces, thus low mechanical reliability. The best mechanical performance (high rupture time ((5498.85 s), low strain rate, and stress exponent (9.48)) has been reported for the 0.5 wt.% of Bi addition to the as-cast eutectic alloy which is strongly related to its high structural stability compared to that for the other additions. So, and from the mechanical point of view, the Sn-0.7Cu-0.5Bi alloy is recommended to be the most mechanical reliable alloy for the large-scale production and processing soldering and electronic assembly.

References

- [1] S. Farina, C. Morando, Comparative corrosion behaviour of different Sn-based solder alloys, *J. Mater. Sci. Mater. Electron.* 26 (2014) 464–471. doi:10.1007/s10854-014-2422-0
- [2] M.S. Gumaan, Chromium improvements on the mechanical performance of a rapidly solidified eutectic Sn–Ag alloy, *J. Mater. Sci. Mater. Electron.* 31 (2020) 10731–10737. doi:10.1007/s10854-020-03623-0
- [3] R. Mostafa, M. Kamal, E.A.M. Ali, M.S. Gumaan, Microstructural and mechanical characterization of melt spun process Sn- 3 . 5Ag and Sn-3 . 5Ag-xCu lead-free solders for low cost electronic assembly, *Mater. Sci. Eng. A.* 690 (2017) 446–452. doi:10.1016/j.msea.2017.03.022
- [4] R.M. Shalaby, M. Kamal, E.A.M. Ali, M.S. Gumaan, Design and Properties of New Lead-Free Solder Joints Using Sn-3.5Ag-Cu Solder, *Silicon.* 10 (2018) 1861–1871. doi:10.1007/s12633-017-9690-2
- [5] J.Y. Tsai, Y.C. Hu, C.M. Tsai, C.R. Kao, A study on the reaction between Cu and Sn3.5Ag solder doped with small amounts of Ni, *J. Electron. Mater.* 32 (2003) 1203–1208. doi:10.1007/s11664-003-0012-7
- [6] A.-A. Bogno, J.E. Spinelli, C.R.M. Afonso, H. Henein, Microstructural and mechanical properties analysis of extruded Sn–0.7Cu solder alloy, *J. Mater. Res. Technol.* 4 (2015) 84–92. doi:10.1016/j.jmrt.2014.12.005
- [7] R.M. Shalaby, Indium, chromium and nickel-modified eutectic Sn–0.7 wt% Cu lead-free solder rapidly solidified from molten state, *J. Mater. Sci. Mater. Electron.* 26 (2015) 6625–6632. doi:10.1007/s10854-015-3261-3
- [8] D.R. Frear, J.W. Jang, J.K. Lin, C. Zhang, Pb-free solders for flip-chip interconnects, *JOM.* 53 (2001) 28–33. doi:10.1007/s11837-001-0099-3
- [9] F. Tai, F. Guo, Z.D. Xia, Y.P. Lei, Y.F. Yan, J.P. Liu, Y.W. Shi, Processing and creep properties of Sn-Cu composite solders with small amounts of nanosized Ag reinforcement additions, *J. Electron. Mater.* 34 (2005) 1357–1362. doi:10.1007/s11664-005-0190-6
- [10] J. Shen, Y.C. Liu, H.X. Gao, Formation of bulk Cu₆Sn₅ intermetallic compounds in Sn-Cu lead-free solders during solidification, *J. Mater. Sci.* 42 (2007) 5375–5380. doi:10.1007/s10853-006-0892-z
- [11] M. Zhao, L. Zhang, Z.Q. Liu, M.Y. Xiong, L. Sun, Structure and properties of Sn-Cu lead-free solders in electronics packaging, *Sci. Technol. Adv. Mater.* 20 (2019) 421–444. doi:10.1080/14686996.2019.1591168
- [12] L. Yang, Y. Zhang, C. Du, J. Dai, N. Zhang, Effect of aluminum concentration on the microstructure and mechanical properties of Sn-Cu-Al solder alloy, *Microelectron. Reliab.* 55 (2015). doi:10.1016/j.microrel.2014.12.017

- [13] S.-H. Huh, K.-S. Kim, K. Sukanuma, Effect of Ag Addition on the Microstructural and Mechanical Properties of Sn-Cu Eutectic Solder, *Mater. Trans.* 42 (2001) 739–744. doi:10.2320/matertrans.42.739
- [14] M. Sahin, T. Sensoy, E. Cadirli, Microstructural evolution and mechanical properties of Sn-Bi-Cu ternary eutectic alloy produced by directional solidification, *Mater. Res.* 21 (2018) 1–10. doi:10.1590/1980-5373-mr-2017-0901
- [15] A.A. El-Daly, A.E. Hammad, Enhancement of creep resistance and thermal behavior of eutectic Sn-Cu lead-free solder alloy by Ag and In-additions, *Mater. Des.* 40 (2012) 292–298. doi:10.1016/j.matdes.2012.04.007
- [16] E.B.; C.A.H.; J.B.; R.D.P.; R.W. Gedney, *Lead-Free Electronics: iNEMI Projects Lead to Successful Manufacturing*, Wiley-IEEE Press, 2007. https://books.google.com/books?id=GPS-BmbwWBgC&pg=PA16&lpg=PA16&dq=Sn-Cu+has+the+lowest+cost+among+several+kinds+of+lead-free+solder&source=bl&ots=JvCXeFjFnB&sig=ACfU3U2pA-XM_xgBjXr8jPUp4lt5z2p63w&hl=en&sa=X&ved=2ahUKewijYbTu6zqAhUB4YUKHUbpB0oQ6AEwAHoECA (accessed July 1, 2020).
- [17] S. Li, X. Wang, Z. Liu, Y. Jiu, S. Zhang, J. Geng, X. Chen, S. Wu, P. He, W. Long, Corrosion behavior of Sn-based lead-free solder alloys: a review, *J. Mater. Sci. Mater. Electron.* 31 (2020) 9076–9090. doi:10.1007/s10854-020-03540-2
- [18] M. Kamal, U. Mohammad, *A review: chill-block melt spin technique, theories & applications*, 2012.
- [19] G. Saad, S.A. Fayek, A. Fawzy, H.N. Soliman, G. Mohammed, Deformation characteristics of Al-4043 alloy, *Mater. Sci. Eng. A.* 527 (2010) 904–910. doi:10.1016/j.msea.2009.09.018
- [20] M.M. Jubair, M.S. Gumaan, R.M. Shalaby, Reliable Sn-Ag-Cu lead-free melt-spun material required for high-performance applications, *Zeitschrift Fur Krist. - Cryst. Mater.* 234 (2019) 757–767. doi:10.1515/zkri-2019-0040
- [21] J. Shen, Y.C. Liu, H.X. Gao, Formation of bulk Cu₆Sn₅ intermetallic compounds in Sn-Cu lead-free solders during solidification, *J. Mater. Sci.* 42 (2007) 5375–5380. doi:10.1007/s10853-006-0892-z
- [22] B. Chalmers, *Principles of Solidification*, in: *Appl. Solid State Phys.*, Springer US, 1970: pp. 161–170. doi:10.1007/978-1-4684-1854-5_5
- [23] B.D. Cullity, *Elements of X-ray Diffraction*, (Addison-Wesely, Reading, 1978). (1978) 248.

- [24] M. Tanaka, T. Sasaki, T. Kobayashi, K. Tatsumi, Improvement in drop shock reliability of Sn-1.2Ag-0.5Cu BGA interconnects by Ni addition, in: Proc. - Electron. Components Technol. Conf., 2006: pp. 78–84. doi:10.1109/ECTC.2006.1645629
- [25] G.. Williamson, W.. Hall, X-ray line broadening from filed aluminium and wolfram, *Acta Metall.* 1 (1953) 22–31. doi:10.1016/0001-6160(53)90006-6
- [26] A. Inoue, H.S. Chen, J.T. Krause, T. Masumoto, M. Hagiwara, Young's modulus of Fe-, Co-, Pd- and Pt-based amorphous wires produced by the in-rotating-water spinning method, *J. Mater. Sci.* 18 (1983) 2743–2751. doi:10.1007/BF00547591
- [27] J. Cai, J. Lin, J. Wilsius, Modelling phase transformations in hot stamping and cold die quenching of steels, in: *Microstruct. Evol. Met. Form. Process.*, Elsevier, 2012: pp. 210–236. doi:10.1533/9780857096340.2.210
- [28] M.S.G. and R.M.S. Sanaa Razzaq Abbas, Chromium effects on the microstructural, mechanical and thermal properties of a rapidly solidified eutectic Sn-Ag alloy, *Solder. Surf. Mt. Technol.* 32 (2019) 137–145.
- [29] M.S. Gumaan, R.M. Shalaby, M.K. Mohammed Yousef, E.A.M. Ali, E.E. Abdel-Hady, Nickel effects on the structural and some physical properties of the eutectic Sn-Ag lead-free solder alloy, *Solder. Surf. Mt. Technol.* 31 (2019) 40–51. doi:10.1108/SSMT-03-2018-0009
- [30] M.S. Gumaan, R.M. Shalaby, E.A.M. Ali, M. Kamal, Copper effects in mechanical, thermal and electrical properties of rapidly solidified eutectic Sn-Ag alloy, *J. Mater. Sci. Mater. Electron.* 29 (2018) 8886–8894. doi:10.1007/s10854-018-8906-6
- [31] Liu Mei Lee and Ahmad Azmin Mohamad, Interfacial Reaction of Sn-Ag-Cu Lead-Free Solder Alloy on Cu: A Review, *Adv. Mater. Sci. Eng.* 2013 (2013) 11. <https://www.hindawi.com/journals/amse/2013/123697/> (accessed July 1, 2020).
- [32] A.F. Abd El-Rehim, H.Y. Zahran, A.M. Yassin, Microstructure evolution and tensile creep behavior of Sn-0.7Cu lead-free solder reinforced with ZnO nanoparticles, *J. Mater. Sci. Mater. Electron.* 30 (2019) 2213–2223. doi:10.1007/s10854-018-0492-0
- [33] R. Mahmudi, A.R. Geranmayeh, H. Noori, G. Nayyeri, F. Pishbin, Creep of dilute tin based lead free solder alloys as replacements of Sn-Pb solders, *Mater. Sci. Technol.* 24 (2008) 803–808. doi:10.1179/174328408X307274
- [34] A. De La Torre, P. Adeva, M. Aballe, Indentation creep of lead and lead-copper alloys, *J. Mater. Sci.* 26 (1991) 4351–4354. doi:10.1007/BF00543650